



Numerical solving of multi- term time fractional diffusion-wave equations using shifted Gegenbauer spectral collocation method

Mahboubeh Molavi-Arabshahi*, Jalil Rashidinia, and Shiva Tanoomand

School of Mathematics and Computer Science, Iran University of Science and Technology, Narmak, Tehran 16844, Iran.

Abstract

In this paper, we present a numerical method to approximate the solution of the multi-term time fractional diffusion-wave equation (M-TFDWE). The proposed method represents the solution as a sum of shifted Gegenbauer polynomials (SGP) with unknown coefficients. By using the operational matrix of fractional integration and integer derivatives based on SGPs, the M-TFDWE is converted into a system of algebraic equations. The convergence analysis of this numerical method are also discussed. Finally, we provide two examples to illustrate the accuracy of the proposed method.

Keywords. Spectral collocation method, Shifted Gegenbauer polynomial, Time fractional diffusion wave equation.

2010 Mathematics Subject Classification. 65L05, 34K06, 34K28.

1. INTRODUCTION

Fractional calculus extends the concepts of differentiation and integration to non-integer orders. Due to the non-local and memory effects inherent in fractional derivatives, fractional differential equations (FDEs) can more accurately model real-life phenomena than traditional integer-order equations. As a result, many fields such as physics, engineering, and chemistry—including solid mechanics [23], bioengineering [11], and electrochemistry [16] employ fractional order models (for more applications of FDEs, see [5, 18, 26]). Analytical solutions of FDEs are often difficult to find, prompting the development of various numerical methods such as finite difference and meshless methods [10, 13–15, 17], the operational matrix method [28, 30], the collocation method [19, 24, 27], and wavelets [8, 25].

Recently, spectral methods have gained traction due to their numerous advantages. They offer high numerical accuracy, allowing for precise solutions with a minimal number of degrees of freedom and thus reducing computational costs. Given the non-local and memory effects of fractional operators, global numerical methods like spectral methods are preferred over local methods. Spectral methods can be categorized into Galerkin, tau, and collocation methods, and they typically use orthogonal polynomials such as Jacobi, Gegenbauer, Laguerre, and Hermite polynomials as basis functions. Various researchers have applied spectral methods to solve FDEs. For instance, Yaghoubi et al [31] solved the fractional pantograph partial differential equation using shifted Gegenbauer polynomials (SGPs). Ahmed et al [3] served SGPs as the basis for the tau spectral method in the space-time fractional telegraph equation. Doha et al [6] introduced a Chebyshev-based spectral method, while Gupta and Kumar [7] employed a spectral collocation method for the fractional mobile-immobile advection-dispersion equation. Rashidinia and Mohmedi [22] used a spectral method for solving parabolic fractional partial differential equations and Abo-Gabal et al.[2] proposed a spectral tau method for time fractional partial differential equations. Pourbabaee and Saadatmandi [20] introduced the Bernoulli-based spectral tau approach for distributed time fractional partial differential equations, and Abbaszadeh et al.[1] described a spectral collocation method for the space fractional reaction-diffusion equation.

Received: 04 May 2024 ; Accepted: 08 October 2024.

* Corresponding author. Email: molavi@iust.ac.ir .

In this paper, we concentrate on the multi-term time fractional diffusion-wave equation (M-TFDWE):

$${}_0^c D_t^\alpha u(x, t) + \sum_{l=1}^m c_l {}_0^c D_t^{\alpha_l} u(x, t) = u_{xx}(x, t) + f(x, t) \quad (x, t) \in [0, 1] \times [0, 1], \quad (1.1)$$

subjected to conditions

$$u(x, 0) = \tau_1(x), \quad u_t(x, 0) = \tau_2(x), \quad (1.2)$$

$$u(a, t) = g_1(t), \quad u(b, t) = g_2(t), \quad (1.3)$$

where $1 < \alpha_1 < \alpha_2 < \dots < \alpha_m < \alpha < 2$, $c_l \geq 0$ $l = 1, 2, \dots, m$. In (1.1), $u(x, t)$ is the unknown function and $f(x, t)$ is a smooth function, $\tau_1(x), \tau_2(x), g_1(t), g_2(t)$ are continuous functions. Some numerical approaches have been investigated for numerical solving the M-TFDWE. Kumar et al. [9] presented a numerical method based on the finite difference and a meshless local collocation method. Yaseen et al. [33] introduced a finite difference based on cubic trigonometric B-spline for solving the M-TFDWE. Yang et al. [32] investigated a spectral collocation method (SCM) with convergence analysis. Molavi-Arabshahi et al. [12] proposed the generalized Laguerre SCM for the M-TFDWE. Heydari et al. [8] applied the Legendre wavelet for the time fractional diffusion-wave equation (TFDWE). Rashidinia and Mohmedi [21] proposed a spectral collocation approach based on Legendre polynomials.

In this study, we use a spectral collocation method utilizing Gegenbauer polynomials to solve the M-TFDWE. The solution is approximated by a series of shifted Gegenbauer polynomials (SGPs). By employing the operational matrix of derivatives and fractional integration for these polynomials, we derive a system of algebraic equations. Then, the numerical solution is obtained by solving this system. The structure of this paper is as follows: section 2 reviews some preliminaries on fractional calculus and Gegenbauer polynomials. Section 3 discusses function approximation. The proposed spectral collocation method based on SGPs is developed in section 4. Section 5 covers the convergence analysis of the numerical approach. To demonstrate the effectiveness of the proposed method, two examples are provided in section 6. The conclusion is presented in section 7.

2. PRELIMINARIES AND DEFINITIONS

In this section, we review various definitions and fundamental properties related to fractional integration and differentiation [5, 18], as well as shifted Gegenbauer polynomials [3, 4, 29, 31].

Definition 2.1. The Riemann-Liouville fractional integral of order $\gamma > 0$ of a function $u(t)$ on $t = (0, T]$ is given as:

$${}_0 I_t^\gamma u(t) = \frac{1}{\Gamma(\gamma)} \int_0^t (t - \sigma)^{\gamma-1} u(\sigma) d\sigma = \frac{1}{\Gamma(\gamma)} t^{\gamma-1} * u(t), \quad (2.1)$$

where $*$ denotes the convolution operator.

Definition 2.2. The Caputo fractional derivative of order $\gamma > 0$ of a function $u(t)$ on $t = (0, T]$ is defined as:

$${}_0 D_t^\gamma u(t) = {}_0 I_t^{m-\gamma} D^m u(t) = \frac{1}{\Gamma(m-\gamma)} \int_0^t (t - \sigma)^{m-\gamma-1} u^{(m)}(\sigma) d\sigma, \quad (2.2)$$

where $m = \lceil \gamma \rceil$

These operators have some properties as following:

- ${}_0 I_t^\gamma t^\beta = \frac{\Gamma(\beta+1)}{\Gamma(\beta+\gamma+1)} t^{\beta+\gamma}$ $\beta > -1$,
- ${}_0 I_t^\gamma (c_1 u_1(t) + c_2 u_2(t)) = c_1 {}_0 I_t^\gamma u_1(t) + c_2 {}_0 I_t^\gamma u_2(t)$,
- ${}_0 I_t^\gamma D_{0,t}^\gamma u(t) = u(t) - \sum_{r=0}^{m-1} u^{(r)}(0) \frac{t^r}{r!}$.

Theorem 2.3. Let $q \in [1, \infty)$, $h \in L^1$ and $s \in L^q$. Then $h * s \in L^q$ and

$$\|h * s\|_q \leq \|h\|_1 \|s\|_q. \quad (2.3)$$

Proof. [31]. □



Definition 2.4. ([3, 31]) The well known Gegenbauer polynomials $C_m^\lambda(x)$ of degree m and order $\lambda > \frac{-1}{2}$ defined on the interval $[-1, 1]$ in terms of Jacobi polynomials $J_m^{(\alpha, \beta)}$ are

$$C_m^\lambda(x) = \frac{\Gamma(\lambda + \frac{1}{2})\Gamma(m + 2\lambda)}{\Gamma(2\lambda)\Gamma(m + \lambda + \frac{1}{2})} J_m^{(\lambda - \frac{1}{2}, \lambda - \frac{1}{2})} \quad \lambda \neq 0,$$

some properties of Gegenbauer polynomials are as follows:

- (i) They are orthogonal with respect to the weighted function $w^\lambda(x) = (1 - x^2)^{\lambda - \frac{1}{2}}$.

$$\int_{-1}^1 C_m^\lambda(x) C_n^\lambda(x) w^\lambda(x) dt = \frac{\Gamma(2\lambda + n) \pi 2^{1-2\lambda}}{\Gamma(n + 1)(n + \lambda)(\Gamma(\lambda))^2} \delta_{mn}$$

where δ_{mn} is the Delta-Kronecher function.

- (ii) Gegenbauer polynomials satisfy in the following recurrence relation:

$$(m + 2)C_{m+2}^\lambda(x) = 2(\lambda + m + 1)x C_{m+1}^\lambda(x) - (2\lambda + m)C_m^\lambda(x),$$

where $C_0^\lambda(x) = 1, C_1^\lambda(x) = 2\lambda x$.

By using the new variable $x = 2t - 1$, we can get the shifted Gegenbauer polynomials on the interval $[0, 1]$ as follows:

$$C_m^\lambda(t) = \frac{\Gamma(\lambda + \frac{1}{2})}{\Gamma(2\lambda)} \sum_{k=0}^m \frac{(-1)^{m-k} \Gamma(m + k + 2\lambda)}{\Gamma(k + \lambda + \frac{1}{2})(m - k)! k!} t^k, \tag{2.4}$$

such that

$$\int_0^1 C_m^\lambda(t) C_n^\lambda(t) w_\lambda(t) dt = \Theta_m^\lambda \delta_{mn},$$

where $w_\lambda(x) = (x - x^2)^{\lambda - \frac{1}{2}}$ and

$$\Theta_m^\lambda = \frac{(\Gamma(\lambda + \frac{1}{2}))^2 \Gamma(m + 2\lambda)}{(\Gamma(2\lambda))^2 (2m + 2\lambda) m!}. \tag{2.5}$$

3. FUNCTION APPROXIMATION

Let $u(t)$ be a square integrable function on $[0, 1]$, so it expresses as a series of the shifted Gegenbauer polynomials as

$$u(t) = \sum_{r=0}^\infty u_r C_r^\lambda(t).$$

In general, $u(t)$ can be approximated by a truncated series of the shifted Gegenbauer polynomials as

$$u(t) \simeq \sum_{r=0}^M u_r C_r^\lambda(t) = L^T(t)U, \tag{3.1}$$

where

$$u_r = \frac{1}{\Theta_r^\lambda} \int_0^1 u(t) C_r^\lambda(t) w_\lambda(t) dt,$$

Θ_r^λ is defined in (2.5) and

$$U = [u_0, u_1, \dots, u_M]^T, \quad L(t) = [C_0^\lambda(t), C_1^\lambda(t), \dots, C_M^\lambda(t)]^T. \tag{3.2}$$

Similarly, for 2D cases, $u(x, t)$ defined on $[0, 1] \times [0, 1]$ may be approximated by a truncated series of the shifted Gegenbauer polynomials as

$$u_M(x, t) = \sum_{m=0}^M \sum_{n=0}^M \nu_{mn} C_m^{(\lambda)}(x) C_n^{(\lambda)}(t) = (L^T(t) \otimes L^T(x)) \vec{U}, \tag{3.3}$$



$$\text{with } U = \begin{bmatrix} \nu_{00} & \nu_{01} & \cdots & \nu_{0M} \\ \nu_{10} & \nu_{11} & \cdots & \nu_{1M} \\ \vdots & \vdots & \cdots & \vdots \\ \nu_{M0} & \nu_{M1} & \cdots & \nu_{MM} \end{bmatrix},$$

and

$$\nu_{mn} = \frac{1}{\Theta_m^\lambda} \frac{1}{\Theta_n^\lambda} \int_0^1 \int_0^1 u_M(x, t) C_m^\lambda(x) C_n^\lambda(t) w_\lambda(x) w_\lambda(t) dx dt, \quad (3.4)$$

for $m = 0, 1, \dots, M$ and $n = 0, 1, \dots, M$.

Definition 3.1. The family of monomials are as follows:

$$w_k = t^k, \quad k = 0, 1, \dots, M,$$

the vector form of m-th monomial functions is defined as

$$\omega(t) = [w_0, w_1, \dots, w_m]. \quad (3.5)$$

Theorem 3.2. Let $L(t)$ and $\omega(t)$ are the vector forms of shifted Gegenbauer polynomials and monomials defined in (3.2) and (3.5), respectively. Then

$$\omega(t) = \rho L(t), \quad (3.6)$$

where

$$\rho = \begin{bmatrix} \rho_{00} & \rho_{01} & \cdots & \rho_{0M} \\ \rho_{10} & \rho_{11} & \cdots & \rho_{1M} \\ \vdots & \vdots & \cdots & \vdots \\ \rho_{M0} & \rho_{M1} & \cdots & \rho_{MM} \end{bmatrix}, \quad (3.7)$$

and

$$\rho_{qj} = \sum_{i=0}^j \frac{2(-1)^{j-i} \Gamma(2\lambda) (j+\lambda) j! \Gamma(i+j+2\lambda) \Gamma(i+q+\lambda+\frac{1}{2})}{(j-i)! i! \Gamma(i+\lambda+\frac{1}{2}) \Gamma(j+2\lambda) \Gamma(i+2\lambda+q+1)}, \quad (3.8)$$

for $q = 0, 1, \dots, M, j = 0, 1, \dots, M$.

Proof. [30] □

Theorem 3.3. ([28]) Let $L(t)$ is the vector form of the shifted Gegenbauer polynomials defined in (3.2). Then:

$${}_0I_t^\alpha L(t) \simeq I_\alpha L(t), \quad (3.9)$$

where $I_\alpha = [\iota(i, j)]_{i, j=0, 1, \dots, M}$ is the $(M+1) \times (M+1)$ matrix and given as follows:

$$\begin{aligned} \iota(i, j) &= \sum_{k=0}^i \sum_{f=0}^j (-1)^{i+j-k-f} \\ &\frac{\Gamma(\lambda + \frac{1}{2}) \Gamma(i+k+2\lambda) j! (j+\lambda) (\Gamma(\lambda))^2 (\Gamma(\lambda + \frac{1}{2}))^2 \Gamma(2\lambda + j + f) \Gamma(\alpha + k + f + \lambda + \frac{1}{2})}{2^{1-4\lambda} \pi \Gamma(2\lambda + j) \Gamma(\lambda + f + \frac{1}{2}) (j-f)! f! \Gamma(2\lambda) \Gamma(\alpha + k + f + 2\lambda + 1)}. \end{aligned}$$

Proof. [28] □



The n-th derivative of the $L(t)$ is defined as follows:

$$\frac{d^n}{dt^n} L(t) = \frac{d^n}{dt^n} \rho^{-1} w(t) = \rho^{-1} D^n \rho L(t), \tag{3.10}$$

where ρ is defined in (3.7)-(3.8), and D is a $(M + 1) \times (M + 1)$ matrix as follows

$$D = \begin{bmatrix} 0 & 0 & \dots & 0 & 0 \\ 1 & 0 & \dots & 0 & 0 \\ \vdots & \vdots & \dots & \vdots & 0 \\ 0 & 0 & \dots & M & 0 \end{bmatrix}.$$

4. THE SHIFTED GEGENBAUER SPECTRAL COLLOCATION METHOD (SGSCM)

In this section, we describe SGSCM for solving the M-TFDWE. The reformulated of the M-TFDWE defined in (1.1) can be constructed using fractional Riemann- Liouville integral of order α as follows:

$$u(x, t) + \sum_{l=1}^m c_l {}_0I_t^{\alpha-\alpha_l} u(x, t) = a {}_0I_t^\alpha u_{xx}(x, t) + H(x, t). \tag{4.1}$$

Where $H(x, t) = (\tau_1(x) + t\tau_2(x))[1 + \sum_{l=1}^m c_l \frac{t^{\alpha-\alpha_l}}{\Gamma(\alpha-\alpha_l+1)}] + {}_0I_t^\alpha f(x, t)$

For using the spectral collocation method, at the first step $u(x, t)$ is approximated by terms of shifted Gegenbauer polynomials as given in (3.3). Then, we have:

$${}_0I_t^\alpha u_{xx}(x, t) \simeq \sum_{i=0}^M \sum_{j=0}^M u_{ij} \frac{d^2}{dx^2} C_i^{(\lambda)}(x) {}_0I_t^\alpha C_j^{(\lambda)}(t) = (L^T(t) I_\alpha^T \otimes L^T(x) D_2^T) \vec{U},$$

using properties of the Kronecker product, we get

$${}_0I_t^\alpha u_{xx}(x, t) \simeq (L^T(t) \otimes L^T(x))(I_\alpha^T \otimes D_2^T) \vec{U}, \tag{4.2}$$

then, for $l = 1, \dots, m$

$$\begin{aligned} {}_0I_t^{\alpha-\alpha_l} u(x, t) &\simeq \sum_{i=0}^M \sum_{j=0}^M u_{ij} C_i^{(\lambda)}(x) {}_0I_t^{\alpha-\alpha_l} C_j^{(\lambda)}(t) = (L^T(t) I_{\alpha-\alpha_l}^T \otimes L^T(x) I_{M+1}^T) \vec{U} \\ &= (L^T(t) \otimes L^T(x))(I_{\alpha-\alpha_l}^T \otimes I_{M+1}^T) \vec{U}, \end{aligned} \tag{4.3}$$

where I_{M+1} is the identity matrix of order $M+1$. Finally, let $H(x,t)$ can be written as a series of SGPs, so

$$H(x, t) \simeq H_M(x, t) = \sum_{i=0}^M \sum_{j=0}^M H_{ij} C_i^\lambda(x) C_j^\lambda(x) = (L^T(t) \otimes L^T(x)) \vec{H}, \tag{4.4}$$

where

$$H_{ij} = \frac{1}{\Theta_m^\lambda} \frac{1}{\Theta_n^\lambda} \int_0^1 \int_0^1 H_M(x, t) C_m^\lambda(x) C_n^\lambda(t) w_\lambda(x) w_\lambda(t) dx dt, \tag{4.5}$$

By replacing (3.3), (4.2),(4.3), and (4.4) in relation (4.1), the residual function $R_M(x, t)$ is given as follows:

$$\begin{aligned} R_M(x, t) &= \left[(L^T(t) \otimes L^T(x)) + \sum_{l=1}^m (L^T(t) \otimes L^T(x))(I_{\alpha-\alpha_l}^T \otimes I_{M+1}^T) - (L^T(t) \otimes L^T(x))(I_\alpha^T \otimes D_2^T) \right] \vec{U} \\ &\quad - (L^T(t) \otimes L^T(x)) \vec{H}. \end{aligned} \tag{4.6}$$

We can generate $(M + 1)(M - 1)$ equations as follows

$$R_M(x_m, t_n) = 0, \quad m = 2, 3, \dots, M, \quad n = 1, 2, \dots, M + 1, \tag{4.7}$$



where $\{x_m\}_{m=1}^{M+1}$ and $\{t_n\}_{n=1}^{M+1}$ are Legendre-Gauss-Lobatto nodes (LGLs). Then, substituting (3.3) in (1.3), and using LGLs as follows

$$(L^T(t_n) \otimes L^T(x_1))\vec{U} = g_1(t_n) \quad n = 1, 2, \dots, M+1, \quad (4.8)$$

$$(L^T(t_n) \otimes L^T(x_{M+1}))\vec{U} = g_1(t_n) \quad n = 1, 2, \dots, M+1, \quad (4.9)$$

we get $2(M+1)$ equations. Finally, using (4.7) - (4.9), we can obtain \vec{U} by solving the linear system of equations as

$$A\vec{U} = \vec{b}.$$

5. CONVERGENCE ANALYSIS

In this section, we study the error of the numerical approach defined in section 4. In error analysis, the usual procedure is the comparison of the numerical solution u_N with an appropriate orthogonal projection $P_N u$ of the exact solution u in suitable Sobolev spaces.

Let \mathcal{P}_M is the set of polynomials of degree up to M . The orthogonal projection is defined as $P_M : L^2_{w_\lambda}(\Lambda) \mapsto \mathcal{P}_M$ such that

$$(P_M u - u, v) = 0 \quad \forall v \in \mathcal{P}_M. \quad (5.1)$$

To measure the truncation error of $P_M u - u$, we introduce following spaces.

Definition 5.1. ([3]) Let $\Lambda = (0, 1)$ and $w_\lambda(x) = (x - x^2)^{\frac{1}{2}}$. We define the Hilbert space $L^2_{w_\lambda}(\Lambda)$ as

$$L^2_{w_\lambda}(\Lambda) = \left\{ u : \Lambda \mapsto \mathbb{R} \mid u \text{ is measurable and } \|u\|_{L^2_{w_\lambda}} = \int_\Lambda u^2(x) w_\lambda(x) dx < \infty \right\}. \quad (5.2)$$

Definition 5.2. ([3]) Let $n \in \mathbb{N}$. The weighted Sobolev space $H^n_{w_\lambda}(\Lambda)$ is defined as follows

$$H^n_{w_\lambda}(\Lambda) = \left\{ u \mid \frac{\partial^i}{\partial x^i} u \in L^2_{w_\lambda}(\Lambda) \quad 0 \leq i \leq n \right\}, \quad (5.3)$$

with semi-norm and norm by

$$|u|_{n, w_\lambda} = \left\| \frac{\partial^n}{\partial x^n} u \right\|_{w_\lambda}, \quad \|u\|_{n, w_\lambda} = \left(\sum_{i=0}^n |u|_{i, w_\lambda}^2 \right)^{\frac{1}{2}}. \quad (5.4)$$

Due to [3], for $u \in H^n_{w_\lambda}(\Lambda)$, $\vartheta \leq n$ we have

$$\|P_M u - u\|_{H^\vartheta_{w_\lambda}(\Lambda)} \leq c M^{\varsigma(\vartheta, n)} \|u\|_{H^n_{w_\lambda}(\Lambda)}, \quad (5.5)$$

where

$$\varsigma(\vartheta, n) = \begin{cases} 2\vartheta - n - \frac{1}{2} & \vartheta > 1, \\ \frac{3}{2}\vartheta - n & 0 \leq \vartheta \leq 1, \\ \vartheta - n & \vartheta < 0. \end{cases}$$

Definition 5.3. ([3]) Let $\Omega = \Lambda \times \Lambda$, $\rho_M(x, t) = \text{span} \{C_i^\lambda(x) C_j^\lambda(t), i, j = 0, 1, \dots, M\}$. The Hilbert space $H^{b,a}_{w_\lambda}(\Omega)$ is defined as

$$H^{b,a}_{w_\lambda}(\Omega) = \left\{ u : \Omega \mapsto \mathbb{R} \mid u \text{ is measurable on } \Omega \text{ and } \frac{\partial^{m+n}}{\partial x^m \partial t^n} u \in L^2_{w_\lambda}(\Omega) \quad 0 \leq m \leq b \quad 0 \leq n \leq a \right\}, \quad (5.6)$$

where

$$\|u\|_{H^{b,a}_{w_\lambda}}^2 = \sum_{m=0}^b \sum_{n=0}^a \left\| \frac{\partial^{m+n}}{\partial x^m \partial t^n} u \right\|_{L^2_{w_\lambda}(\Omega)}^2,$$



and $H_{w_\lambda}^{b,0} = L_{w_\lambda}^2(\Lambda_t; H_{w_\lambda}^b(\Lambda_x))$, $H_{w_\lambda}^{0,a} = H_{w_\lambda}^a(\Lambda_t; L_{w_\lambda}^2(\Lambda_x))$ with following norms

$$\|u\|_{H_{w_\lambda}^{b,0}}^2 = \int_0^1 \|u(\cdot, t)\|_{H_{w_\lambda}^b(\Lambda_x)}^2 dt \quad \|u\|_{H_{w_\lambda}^{0,a}}^2 = \sum_{i=0}^a \left\| \frac{\partial^i u}{\partial t^i} \right\|_{L_{w_\lambda}^2(\Omega)}^2. \quad (5.7)$$

Let the orthogonal projection $P_{M,M} : L_{w_\lambda}^2(\Omega) \mapsto \rho_M$, i.e.,

$$P_{M,M}(u(x, t)) = u_M(x, t) \quad \forall u(x, t) \in L_{w_\lambda}^2(\Omega).$$

Then, due to [3], we have

$$\|u - u_M\|_{L_{w_\lambda}^2(\Omega)} \leq c_1 M^{-b} \|u\|_{H_{w_\lambda}^{b,0}} + c_2 M^{-a} \|u\|_{H_{w_\lambda}^{0,a}} \leq M^{\max(-b, -a)} (c_1 \|u\|_{H_{w_\lambda}^{b,0}} + c_2 \|u\|_{H_{w_\lambda}^{0,a}}). \quad (5.8)$$

Now, we will investigate the convergence analysis of the proposed method in the following thmrem.

Theorem 5.4. *Let $u(x, t)$, $u_M(x, t)$ are the exact and numerical solution of the Equation (1.1) subjected to initial and boundary conditions (1.2)- (1.3), and $H(x, t)$ defined in (4.1) can be approximated by a series of GLPs. Then*

$$\|R_M(x, t)\|_{L_{w(\beta)}^2(\Omega)} \longrightarrow 0 \quad (5.9)$$

Proof. $u_M(x, t)$ satisfies at the Equation (4.1) as follows

$$u_M(x, t) + \sum_{l=1}^m c_l {}_0I_t^{\alpha-\alpha_l} u_M(x, t) = {}_0I_t^\alpha \frac{\partial^2}{\partial x^2} u_M(x, t) + H(x, t) + R_M(x, t). \quad (5.10)$$

Subtracting (5.10) and (4.1) we have

$$\|R_M(x, t)\|_{L_{w_\lambda}^2(\Omega)} = \|e_M(x, t) + \sum_{l=1}^m c_l {}_0I_t^{\alpha-\alpha_l} e_M(x, t) - {}_0I_t^\alpha \frac{d^2}{dx^2} e_M(x, t) - H_M(x, t) + H(x, t)\|_{L_{w_\lambda}^2(\Omega)}, \quad (5.11)$$

where $e_M(x, t) = u(x, t) - u_M(x, t)$. From (5.11), we get

$$\begin{aligned} \|R_M(x, t)\|_{L_{w_\lambda}^2(\Omega)} &\leq \|e_M(x, t)\|_{L_{w_\lambda}^2(\Omega)} + \sum_{l=1}^m |c_l| \|{}_0I_t^{\alpha-\alpha_l} e_M(x, t)\| + \|{}_0I_t^\alpha \frac{d^2}{dx^2} e_M(x, t)\|_{L_{w_\lambda}^2(\Omega)} \\ &\quad + \|H_M(x, t) - H(x, t)\|_{L_{w_\lambda}^2(\Omega)}. \end{aligned} \quad (5.12)$$

Now, we find the boundary for each terms of right side (5.12). By (5.8), for sufficiently large M, the following relation can be concluded

$$\|e_M(x, t)\|_{L_{w_\lambda}^2(\Omega)} \longrightarrow 0, \quad (5.13)$$

and

$$\sum_{l=1}^m |c_l| \|{}_0I_t^{\alpha-\alpha_l} e_M(x, t)\|_{L_{w_\lambda}^2(\Omega)} \leq C_1 \sum_{l=1}^m \|{}_0I_t^{\alpha-\alpha_l} e_M(x, t)\|_{L_{w_\lambda}^2(\Omega)}, \quad (5.14)$$

for every $l = 1, \dots, m$, using (2.1), (2.3), and (5.8)

$$\|{}_0I_t^{\alpha-\alpha_l} e_M(x, t)\|_{L_{w_\lambda}^2(\Omega)} \leq \frac{1}{\Gamma(\alpha-\alpha_l)} \|t^{\alpha-\alpha_l-1}\|_1 \|e_M(x, t)\|_{L_{w_\lambda}^2(\Omega)} \leq C_2 \|e_M(x, t)\|_{L_{w_\lambda}^2(\Omega)} \quad (5.15)$$

using (5.8), we conclude $\|e_M(x, t)\|_{L_{w_\lambda}^2(\Omega)} \longrightarrow 0$. So, we have

$$\|{}_0I_t^{\alpha-\alpha_r} e_M(x, t)\|_{L_{w_\lambda}^2(\Omega)} \longrightarrow 0. \quad (5.16)$$

Then, using (2.1), (2.3) and (5.7) we get

$$\|{}_0I_t^\alpha \frac{d^2}{dx^2} e_M(x, t)\|_{L_{w_\lambda}^2(\Omega)} \leq \frac{1}{\Gamma(\alpha)} \|t^{\alpha-1}\|_1 \quad \left\| \frac{d^2}{dx^2} e_M(x, t) \right\|_{L_{w_\lambda}^2(\Omega)} \leq C_2 \|e_M(x, t)\|_{H_{w_\lambda}^{0,2}},$$



then using (5.5), for sufficiently large M , we get $\|e_M(x, t)\|_{H_{w_\lambda}^{0,2}} \rightarrow 0$ and

$$\|{}_0I_t^\alpha \frac{d^2}{dx^2} e_M(x, t)\|_{L_{w_\lambda}^2(\Omega)} \rightarrow 0. \quad (5.17)$$

From (5.8), for $H(x, t) \in L_{w_\lambda}^2(\Omega)$, we can conclude

$$\|H_M(x, t) - H(x, t)\|_{L_{w_\lambda}^2(\Omega)} \leq c_1 M^{-m} \|H\|_{H_{w_\lambda}^{m,0}(\Omega)} + c_2 M^{-n} \|H\|_{H_{w_\lambda}^{0,n}(\Omega)},$$

so, when M is enough large

$$\|H_M(x, t) - H(x, t)\|_{L_{w_\lambda}^2(\Omega)} \rightarrow 0, \quad (5.18)$$

by using (5.13), (5.16), (5.17), and (5.18) in (5.12) the result can be obtained. \square

6. NUMERICAL EXAMPLES

In this section, we evaluate the efficiency of the shifted Gegenbauer spectral collocation method. We compute the following errors:

$$L_2 = \left(\sum_{m=1}^{M+1} |u(x_m, T) - u_M(x_m, T)|^2 \right)^{\frac{1}{2}},$$

$$L_\infty = \max(|u(x_m, t_n) - u_M(x_m, t_n)|),$$

where $\{u(x_m, t_n)\}_{m,n=1,\dots,M+1}$ and $\{u_M(x_m, t_n)\}_{m,n=1,\dots,M+1}$ are the exact and numerical solutions at the collocation nodes, respectively. All computations were performed using Matlab 2016 on a laptop with an Intel Core i5-2450M CPU @ 2.50 GHz, 2 cores. In the following two examples, we consider two sets of collocation nodes for comparison:

- Gauss-Legendre lobatto nodes (GLL),
- Equal spaced nodes (Es).

Example 6.1. Consider the following equations as

$${}_c D_t^\alpha u(x, t) = \frac{\partial^2 u(x, t)}{\partial x^2} + q(x, t) \quad (x, t) \in (0, 1) \times [0, 1],$$

with initial conditions

$$u(x, 0) = 0, \quad u_t(x, 0) = 0,$$

and boundary conditions

$$u(0, t) = 0, \quad u(1, t) = 0,$$

where

$$q(x, t) = 6 \frac{t^{3-\alpha}}{\Gamma(4-\alpha)} x^{1+\alpha}(1-x) - t^3(1+\alpha)x^{\alpha-1}(\alpha - (2+\alpha)x),$$

and $u(x, t) = t^3 x^{1+\alpha}(1-x)$.

In Table 1, the L_2 -errors and L_∞ -errors for $\lambda = 1.25$ and various α values using GLL nodes are presented. Table 2 provides the L_2 -errors and L_∞ -errors for $\lambda = 1.25$ and different α values using Es nodes. A comparison between Table 1 and Table 2 indicates that employing GLL nodes as collocation points yields more accurate results than using Es nodes. Table 3 displays the L_∞ -errors and CPU time for $\lambda = 0.25, \alpha = 1.5$ and $\lambda = 1.25, \alpha = 1.5$. Figure 1 shows the plot of numerical solutions for $\lambda = 1.5, \alpha = 1.7, 1.8, 1.9, 2$, with $N = 6$ and $t = 1$. Table 4 lists the absolute errors for $\lambda = 1.5, \alpha = 1.7, 1.8, 1.9, 2$, with $N = 6$ and $t = 1$. The results demonstrate that the numerical method performs better as the fractional order ($1 < \alpha < 2$) approaches the integer order ($\alpha = 2$). In Figure 2, the logarithmic representation of the L_∞ -errors for $\alpha = 1.1, 1.9$ is plotted.



TABLE 1. L_∞ -error and L_2 -error at GLL nodes for Example 6.1.

M	$\alpha = 1.1, \lambda = 1.25$		$\alpha = 1.5, \lambda = 1.25$		$\alpha = 1.9, \lambda = 1.25$	
	L_∞	L_2	L_∞	L_2	L_∞	L_2
3	0.0160	0.0120	0.0173	0.0173	0.0154	0.0154
4	0.0061	0.0016	0.0084	0.0041	0.0083	0.0087
5	$2.4912e-4$	$2.5611e-4$	$7.9850e-4$	$5.5410e-4$	0.0018	0.0020
6	$1.2958e-4$	$1.4066e-4$	$1.6839e-4$	$1.8581e-4$	$2.9299e-5$	$3.4604e-5$
7	$6.1212e-5$	$6.8441e-5$	$7.1787e-5$	$7.7013e-5$	$9.2215e-6$	$1.0027e-5$
8	$3.4166e-5$	$4.0607e-5$	$3.4889e-5$	$3.8682e-5$	$3.8071e-6$	$4.1441e-6$
9	$2.0013e-5$	$2.4799e-5$	$1.8361e-5$	$2.1234e-5$	$1.8125e-6$	$1.9956e-6$

TABLE 2. L_∞ -error and L_2 -error at Es nodes for Example 6.1.

M	$\alpha = 1.1, \lambda = 1.25$		$\alpha = 1.5, \lambda = 1.25$		$\alpha = 1.9, \lambda = 1.25$	
	L_∞	L_2	L_∞	L_2	L_∞	L_2
3	0.0160	0.0120	0.0173	0.0173	0.0154	0.0154
4	0.0060	0.0016	0.0071	0.0084	0.0123	0.0127
5	$7.2778e-4$	$7.8567e-4$	0.0015	0.0016	0.0010	0.0012
6	$4.3162e-4$	$5.6797e-4$	$7.2949e-4$	$9.4861e-4$	$1.3698e-4$	$1.6383e-4$
7	$2.4354e-4$	$3.1041e-4$	$3.7244e-4$	$4.5163e-4$	$6.1146e-5$	$7.0266e-5$
8	$1.6438e-4$	$2.3981e-4$	$2.2450e-4$	$3.1049e-4$	$3.2304e-5$	$4.0422e-5$
9	$1.1255e-4$	$1.6260e-4$	$1.4191e-4$	$1.9304e-4$	$1.8811e-5$	$2.3787e-5$

Example 6.2. Consider the time fractional diffusion-wave equation

$${}^c_0D_t^\alpha \nu(x, t) + {}^c_0D_t^{\alpha_1} \nu(x, t) = \frac{\partial^2}{\partial x^2} \nu(x, t) + g(x, t) \quad (x, t) \in (0, 1) \times [0, 1],$$

with homogeneous initial and boundary conditions and

$$g(x, t) = \left(\frac{6t^{3-\alpha}}{\Gamma(4-\alpha)} + \frac{6t^{3-\alpha_1}}{\Gamma(4-\alpha_1)} \right) \sin(\pi x) + (\pi^2 t^3) \sin(\pi x).$$

Where $\nu(x, t) = t^3 \sin(\pi x)$.

Table 5 compares the L_∞ -errors of our proposed method for $\lambda = -0.25$ with the method used in [21], showing that our method is more accurate. Table 6 presents the L_∞ -errors and CPU times of the proposed method for $\alpha = 1.5$, $\alpha_1 = 1.2$, with $\lambda = -\frac{1}{4}$ and $\lambda = 1.5$. Figure 3 displays the logarithmic representation of L_∞ -errors for $\lambda = -0.25$, $\alpha = 1.9$, $\alpha_1 = 1.3$, and $\alpha = 1.7$, $\alpha_1 = 1.2$. Figure 4 shows the logarithmic representation of L_∞ -errors for $\lambda = -0.25$, $\lambda = 1.5$, $\alpha = 1.5$, and $\alpha_1 = 1.2$. In Table 7, the L_∞ -errors are given for Es nodes and GLL nodes at $\alpha = 1.1$, $\alpha_1 = 1.2$, $\lambda = -0.25$ and $\alpha = 1.9$, $\alpha_1 = 1.2$, $\lambda = -0.25$, demonstrating that GLL nodes provide more accurate results than Es nodes.

7. CONCLUSION

In this paper, we presented a spectral method utilizing shifted Gegenbauer polynomials (SGP) for numerically solving the multi-term time fractional diffusion-wave equation (M-TFDWE). In this approach, the exact solution is expressed in terms of SGPs. By employing the fractional Riemann-Liouville integral operator, the M-TFDWE is reformulated into its integrated form. Then, using the operational matrix of fractional integration and integer derivative along with collocation nodes, we derive a system of algebraic equations. The use of operational matrices of



TABLE 3. L_∞ -errors and CPU-time for Example 6.1.

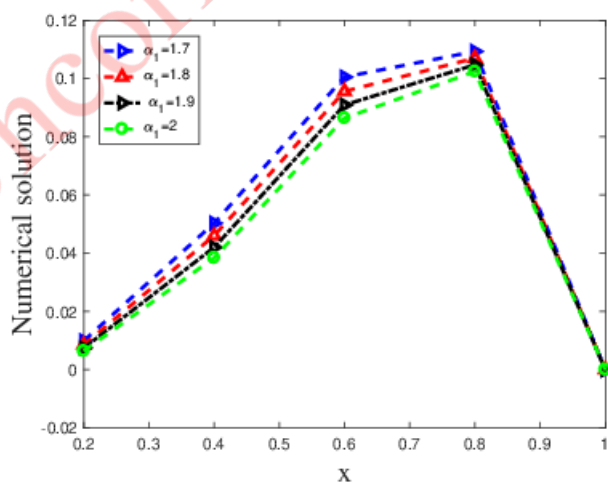
M	$\alpha = 1.5, \lambda = 0.25$		$\alpha = 1.5, \lambda = 1.25$	
	L_∞	CPU-time	L_∞	CPU-time
3	0.0184	0.11s	0.0173	0.12s
4	0.0045	0.12s	0.0084	0.13s
5	$4.7599e-4$	0.15s	$7.9850e-4$	0.15s
6	$1.6556e-4$	0.17s	$1.6839e-4$	0.16s

TABLE 4. Absolute errors at different values of α , $\lambda = 1.5$ and $t = 1$ for Example 6.1.

x_i	$\alpha = 1.7$	$\alpha = 1.8$	$\alpha = 1.9$	$\alpha = 2$
0.2	$4.3922e-4$	$2.9059e-4$	$1.3727e-4$	$1.7000e-14$
0.4	$2.3480e-4$	$1.4653e-4$	$6.4337e-5$	$4.5582e-14$
0.6	$1.8190e-4$	$9.4368e-5$	$3.6684e-5$	$4.9502e-14$
0.8	$1.8948e-4$	$1.1723e-4$	$5.2303e-5$	$2.8010e-13$
1	$1.1364e-16$	$1.2581e-17$	$1.1652e-19$	$9.8084e-17$

TABLE 5. Comparison of GLSCM with $\lambda = \frac{-1}{4}$ with [21] for Example 6.2.

M	$\alpha = 1.9, \alpha_1 = 1.3$		$\alpha = 1.7, \alpha_1 = 1.2$	
	GLSCM	[21]	GLSCM	[21]
4	0.0045	$3.8806e-3$	0.0051	$4.0956e-3$
5	0.0015	$2.001e-3$	0.0015	$2.0625e-3$
6	$2.8581e-5$	$6.5229e-5$	$2.6437e-5$	$6.6232e-5$
7	$7.3878e-6$	$3.0780e-5$	$7.9742e-6$	$3.1689e-5$
8	$4.6386e-7$	$2.4718e-6$	$4.5421e-7$	$1.9346e-6$
9	$1.9323e-7$	$2.6136e-7$	$2.2402e-7$	$4.3888e-7$

FIGURE 1. Represent of the numerical solution at $\lambda = 1.5$, $N = 6$ and $t = 1$ for Example 6.1.

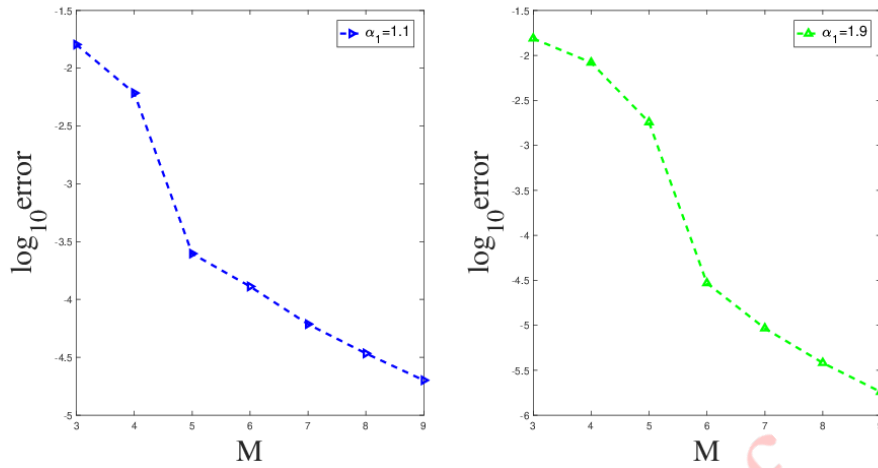


FIGURE 2. Logarithmic representation of the max absolute error at $\lambda = 1.25$ for Example 6.1.

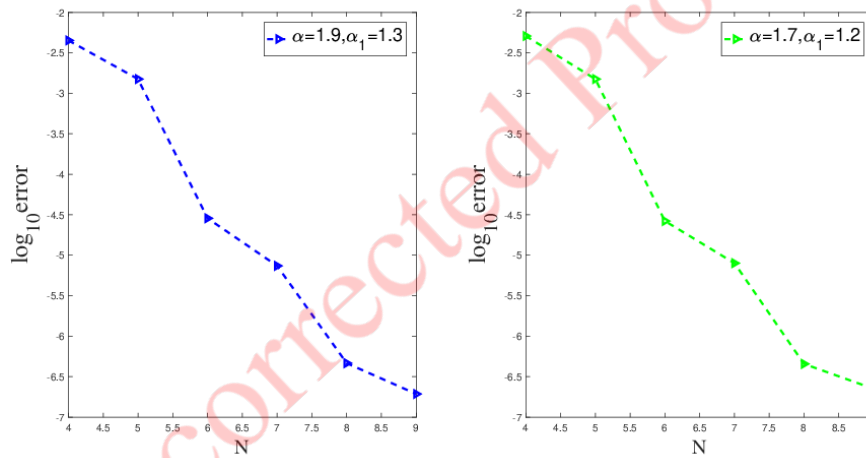


FIGURE 3. Logarithmic representation of the max absolute error at $\lambda = -0.25$ for Example 6.2.

TABLE 6. L_∞ -error, CPU-time at $\alpha = 1.5, \alpha_1 = 1.2$ and various values of λ for Example 6.2.

M	$\lambda = -0.25$		$\lambda = 1.5$	
	L_∞	CPU-time	L_∞	CPU-time
3	0.0607	0.053s	0.1348	0.052s
4	0.0052	0.056s	0.0261	0.053s
5	0.0014	0.079s	0.0029	0.077s
6	$2.5396e-5$	0.096s	$7.4985e-5$	0.11s
7	$8.4211e-6$	0.16s	$1.2512e-5$	0.15s
8	$4.7640e-7$	0.21s	$3.9986e-6$	0.22s
9	$2.7965e-7$	0.31s	$2.8039e-6$	0.28s



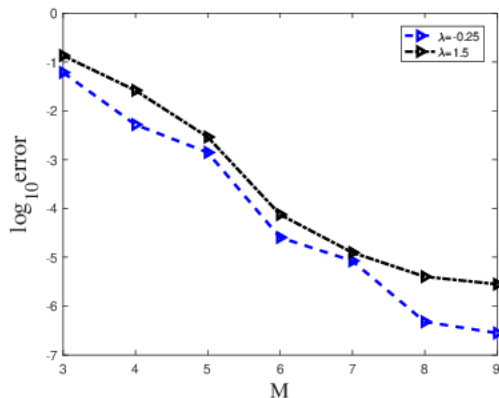


FIGURE 4. Logarithmic representation of the max absolute error at $\alpha = 1.5, \alpha_1 = 1.2$ for Example 6.2.

TABLE 7. L_∞ -error, for Es nodes and GLL nodes at $\lambda = -0.25$ for Example 6.2.

M	$\alpha = 1.1, \alpha_1 = 1.2$		$\alpha = 1.9, \alpha_1 = 1.2$	
	GLL	Es	GLL	Es
3	0.0977	0.0977	0.0567	0.0567
4	0.0023	0.0435	0.0046	0.0265
5	0.0013	0.0044	0.0015	0.0031
6	$2.5983e-5$	0.0027	$2.8136e-5$	0.0020
7	$9.4981e-6$	$1.1736e-4$	$7.7265e-6$	$9.4888e-5$

SGPs helps reduce computational costs. We also examined the convergence of the numerical solution. Finally, two examples were solved to demonstrate the efficiency of our proposed method. The numerical illustrations showed that an accurate solution could be achieved with a small number of basis functions.

ACKNOWLEDGEMENTS

We would like to express gratitude to the reviewers and the editor for their valuable feedback and contributions to the improvement of this work.

REFERENCES

- [1] M. Abbaszadeh, A. Bagheri Salec, A. Al-Khafaji, and S. Kamel, *The effect of fractional-order derivative for pattern formation of Brusselator reaction-diffusion model occurring in chemical reactions*, Iranian J. Math. Chem., 14(4) (2023), 243–269.
- [2] H. Abo-Gabal, M. A. Zaky, and E. H. Doha, *Fractional Romanovski-Jacobi tau method for time-fractional partial differential equations with nonsmooth solutions*, Appl. Numer. Math., 182 (2022), 214–234.
- [3] H. F. Ahmed, M. R. A. Moubarak, and W. A. Hashem, *Gegenbauer spectral tau algorithm for solving fractional telegraph equation with convergence analysis*, Pramana., 95(2) (2021).
- [4] W. W. Bell, *Special functions for scientists and engineers*, Dover Publications., 2004.
- [5] K. Diethelm, *The analysis of fractional differential equations: An application-oriented exposition using operators of Caputo type*, Lecture Notes in Mathematics, Springer., (2010).
- [6] E. H. Doha, A. H. Bhrawy, and S. S. Ezz-Eldien, *A Chebyshev spectral method based on operational matrix for initial and boundary value problems of fractional order*, Comput. Math. Appl., 62(5) (2011), 2364–2373.



- [7] R. Gupta and S. Kumar, *Chebyshev spectral method for the variable-order fractional mobile-immobile advection-dispersion equation arising from solute transport in heterogeneous media*, J. Eng. Math., 142(1) (2023), DOI:10.1007/s10665-023-10288-1.
- [8] M. H. Heydari, M. R. Hooshmandasl, F. M. Ghaini, and C. Cattani, *Wavelets method for the time fractional diffusion-wave equation*, Phys. Lett. A., 379(3) (2015), 71–76.
- [9] A. Kumar, A. Bhardwaj, and B. R. Kumar, *A meshless local collocation method for time fractional diffusion wave equation*, Comput. Math. Appl., 78(6) (2019), 1851–1861.
- [10] Z. Liu, A. Cheng, and X. Li, *A novel finite difference discrete scheme for the time fractional diffusion-wave equation*, Appl. Numer. Math., 134 (2018), 17–30.
- [11] R. Magin, *Fractional calculus in bioengineering*, Crit. Rev. Biomed. Eng., 32(1) (2004), 1–104, doi: 10.1615/critrevbiomedeng.v32.i1.10. PMID: 15248549.
- [12] M. Molavi-Arabshahi, J. Rashidinia, and S. Tanoomand, *An efficient spectral collocation method based on the generalized Laguerre polynomials to multi-term time fractional diffusion-wave equations*, AIP Adv., 14(2) (2024).
- [13] M. Molavi-Arabshahi, J. Rashidinia, and M. Yousefi, *A Novel Hybrid Approach to Approximate fractional Sub-Diffusion Equation*, Comput. Methods Differ. Equ., (2024), 1–12.
- [14] M. Molavi-Arabshahi, J. Rashidinia, and M. Yousefi, *An efficient approach for solving a class of fractional anomalous diffusion equation with convergence*, Phys. Scr., 99 (7) (2024).
- [15] O. Nikan, J. T. Machado, A. Golbabai, and J. Rashidinia, *Numerical evaluation of the fractional Klein-Kramers model arising in molecular dynamics*, J. Comput. Phys., 428 (2021).
- [16] K. B. Oldham, *Fractional differential equations in electrochemistry*, Adv. Eng. Softw., 41(1) (2010), 9–12.
- [17] C. Piret and E. Hanert, *A radial basis functions method for fractional diffusion equations*, J. Comput. Phys., 238 (2013), 71–81.
- [18] I. Podlubny, *Fractional differential equations: an introduction to fractional derivatives, fractional differential equations, to methods of their solution and some of their applications*, Academic Press, Vol. 198, 1998.
- [19] M. Pourbabaee and A. Saadatmandi, *Collocation method based on Chebyshev polynomials for solving distributed order fractional differential equations*, Comput. Methods Differ. Equ., 9(3) (2021), 858–873.
- [20] M. Pourbabaee and A. Saadatmandi, *New operational matrix of Riemann-Liouville fractional derivative of orthonormal Bernoulli polynomials for the numerical solution of some distributed-order time-fractional partial differential equations*, J. Appl. Anal. Comput., 13(6) (2023), 3352–3373.
- [21] J. Rashidinia and E. Mohmedi, *Approximate solution of the multi-term time fractional diffusion and diffusion-wave equations*, Comput. Appl. Math., 39(3) (2020), 1–25.
- [22] J. Rashidinia and E. Mohmedi, *Numerical solution for solving fractional parabolic partial differential equations*, Comput. Methods Differ. Equ., 10(1) (2022), 121–143.
- [23] Y. A. Rossikhin and M. V. Shitikova, *Applications of fractional calculus to dynamic problems of linear and nonlinear hereditary mechanics of solids*, Appl. Mech. Rev., 50(1) (1997), 15–67.
- [24] A. Saadatmandi, A. Khani, and M. R. Azizi, *Numerical calculation of fractional derivatives for the sinc functions via Legendre polynomials*, Math. Interdiscip. Res., 5(2) (2020), 71–86.
- [25] A. Secer and N. Ozdemir, *An effective computational approach based on Gegenbauer wavelets for solving the time-fractional Kdv-Burgers-Kuramoto equation*, Adv. Differ. Equ., 2019 (2019), 1–19.
- [26] R. Shahabifar, M. Molavi-Arabshahi, and O. Nikan, *Numerical analysis of COVID-19 model with Caputo fractional order derivative*, AIP Adv., 14(3) (2024).
- [27] A. Singh and S. Kumar, *A convergent exponential B-spline collocation method for a time-fractional telegraph equation*, Comput. Appl. Math., 42(2) (2023).
- [28] F. Soufivand, F. Soltanian, and K. Mamehrashi, *An operational matrix method based on the Gegenbauer polynomials for solving a class of fractional optimal control problems*, Int. J. Ind. Electron. Control Optim., 4(4) (2021), 475–484.
- [29] G. Szego, *Orthogonal polynomials*, American Mathematical Society, Providence, 107, 1939.
- [30] M. Usman, M. Hamid, T. Zubair, R. U. Haq, W. Wang, and M. B. Liu, *Novel operational matrices-based method for solving fractional-order delay differential equations via shifted Gegenbauer polynomials*, Appl. Math. Comput.,



- 372 (2020).
- [31] S. Yaghoubi, H. Aminikhah, and K. Sadri, *A spectral shifted Gegenbauer collocation method for fractional pantograph partial differential equations and its error analysis*, *Sdhan.*, 48(4) (2023).
 - [32] Y. Yang, Y. Chen, Y. Huang, and H. Wei, *Spectral collocation method for the time fractional diffusion-wave equation and convergence analysis*, *Comput. Math. Appl.*, 73(6) (2017), 1218–1232.
 - [33] M. Yaseen, M. Abbas, T. Nazir, and D. Baleanu, *A finite difference scheme based on cubic trigonometric B-splines for a time fractional diffusion-wave equation*, *Adv. Differ. Equ.*, 2017 (1) (2017), 1–18.

Uncorrected Proof

